EJN fens EUROPEAN JOURNAL OF NEUROSCIENCE

European Journal of Neuroscience, Vol. 38, pp. 3435–3447, 2013 doi:10.1111/ejn.12342

NEUROSYSTEMS

Synaptic gating at axonal branches, and sharp-wave ripples with replay: a simulation study

Nikita Vladimirov, Yuhai Tu and Roger D. Traub
IBM T. J. Watson Research Center, Yorktown Heights, NY, USA

Keywords: CA1, gap junction, hippocampus, place cell

Abstract

Mechanisms of place cell replay occurring during sharp-wave ripples (SPW-Rs) remain obscure due to the fact that ripples *in vitro* depend on non-synaptic mechanisms, presumably via axo-axonal gap junctions between pyramidal cells. We suggest a model of *in vivo* SPW-Rs in which synaptic excitatory post-synaptic potentials (EPSPs) control the axonal spiking of cells in SPW-Rs: ripple activity remains hidden in the network of axonal collaterals (connected by gap junctions) due to conduction failures, unless there is a sufficient dendritic EPSP. The EPSP brings the axonal branching point to threshold, and action potentials from the collateral start to propagate to the soma and to the distal axon. The model coherently explains multiple experimental data on SPW-Rs, both *in vitro* and *in vivo*. The mechanism of synaptic gating leads to the following implication: a sequence of pyramidal cells can be replayed at ripple frequency by the superposition of subthreshold dendritic EPSPs and ripple activity in the axonal plexus. Replay is demonstrated in both forward and reverse directions. We discuss several testable predictions. In general, the mechanism of synaptic gating suggests that pyramidal cells under certain conditions can act like a transistor.

Introduction

The hippocampus is crucially involved in episodic memory and spatial navigation in humans, non-human primates and rodents. The hippocampus in rats maintains three main oscillatory states: theta oscillations (4–10 Hz), which occur during spatial exploration and rapid eye movement sleep; gamma oscillations (20–80 Hz), which are embedded in and modulated by theta; and sharp-wave ripples (SPW-R, 100–250 Hz), which occur during waking immobility, grooming, consummatory behavior, and slow-wave sleep (O'Keefe & Nadel 1978; Buzsáki 1986; Buzsáki *et al.*, 1992). Of special interest are the SPW-Rs, for several reasons: they are the most coherent oscillations in rat hippocampus, with high extracellular amplitude (up to 1 mV), high spatial coherence (over 1 mm), and high frequency (100–250 Hz) (Buzsáki *et al.*, 1992; Ylinen *et al.*, 1995; Chrobak & Buzsáki 1996). Sharp waves in the stratum radiatum of the CA1 region are the result of strong synchronous excitatory input from the CA3 region via Schaffer collaterals (Buzsáki 1986), which triggers, directly or indirectly, transient high-frequency oscillations (ripples) in the CA1.

The reactivation of place cells pairs which were previously co-active during spatial exploration was demonstrated during sleep (Wilson *et al.*, 1994) and cells were shown to fire in the exact or similar temporal order as they had been firing during the exploration (Skaggs *et al.*, 1996; Lee & Wilson 2002). The experience-specific reactivation is strongest during SPW-Rs in slow-wave sleep and quiet wakefulness (Kudrimoti *et al.*, 1999; Nádasdy *et al.*, 1999), and in the occasional SPW-Rs during exploration (O'Neill *et al.*, 2006; Davidson *et al.*, 2009). The reactivation (replay) occurs either before or after the exploration, and it can have forward or reverse order (Foster & Wilson 2006; Diba & Buzsáki 2007). Forward replay occurs at the beginning of runs, suggesting its role in evaluating future trajectories (Diba & Buzsáki 2007), and during post-exploration slow-wave sleep (Skaggs *et al.*, 1996; Lee & Wilson 2002). Reverse replay occurs at the end of a run, when the animal consumes a reward, perhaps linking the trajectory's structure to its outcome (Foster & Wilson 2006; Csicsvari *et al.*, 2007; Diba & Buzsáki 2007). Disruption of SPW-R in awake animals (Jadhav *et al.*, 2012) and during post-training non-rapid eye movement sleep (Girardeau *et al.*, 2009) results in impairment of spatial learning (see also Ego-Stengel & Wilson 2010). In non-disrupted SPW-Rs, a task-related sensory cue biases replay events toward replaying the spatial memory associated with that cue (Bendor & Wilson 2012). Altogether, there is growing evidence that SPW-R and possibly replay can underlie memory consolidation. What is the cellular mechanism of SPW-Rs *in vivo*? What is the mechanism of forward place cell replay? Answers to these questions are complicated by the fact that SPW-Rs, and especially their high-frequency component (ripples) seem to depend on both chemical synapses and non-synaptic mechanisms, at least *in vitro*. Ripples *in vitro* occur in isolated CA1 (Maier *et al.*, 2003; Nimmrich *et al.*, 2005; Maier *et al.*, 2011), which is known to have sparse recurrent synaptic connections between pyramidal cells (PCs) (Deuchars & Thomson 1996). Oscillations in ripple frequency persist in the stratum oriens of CA1 even following separation of the PC layer, presumably from within the PC axonal plexus (Traub *et al.*, 2003). In Draguhn *et al.* (1998), the authors showed that 200 Hz ripples persisted when gamma-

Correspondence: Nikita Vladimirov, as above.
E-mail: nikita.vladimirov@gmail.com

Received 18 April 2013, revised 20 July 2013, accepted 24 July 2013

aminobutyric acid type A ($GABA_A$, alpha-amino-3-hydroxy-5-methyl-4-isoxazolepropionic acid (AMPA)/kainate and *N*-methyl-D-aspartate receptors were blocked pharmacologically, and also when chemical synaptic transmission was blocked by applying low-calcium medium, in all major hippocampal regions. In contrast, ripples were suppressed (reversibly) by application of gap junction blockers, also shown in Maier *et al.* (2003) and Nimmrich *et al.* (2005). There is additional evidence supporting the existence of gap junctions between cortical pyramidal neurons from electrophysiological, pharmacological, and dye coupling data (Church & Baimbridge 1991; Schmitz *et al.*, 2001; Mercer *et al.*, 2006; Hamzei-Sichani *et al.*, 2007; Wang *et al.*, 2010), although it is not yet clear which connexins are involved. The axonal location of those gap junctions is suggested by the fact that somatic or axonal electrical stimulation of one cell can generate a nearly simultaneous (in less than 1 ms) spikelet in a coupled cell (Schmitz *et al.*, 2001; Mercer *et al.*, 2006; Wang *et al.*, 2010) – a notion that is difficult to explain by somato-dendritic gap junctions, but can be readily reproduced in models with axonal gap junctions (Draguhn *et al.*, 1998; Traub *et al.*, 1999; Schmitz *et al.*, 2001). Spikelets (partial spikes) indicate axonally generated action potentials propagating antidromically and failing to invade the soma (Hu *et al.*, 2009). Their fast rise time and high amplitude make them clearly distinguishable from excitatory post-synaptic potentials (EPSPs) and dendritic spikes. Their incidence can be increased by putative axonal gap junctions due to APs in the coupled cell (Draguhn *et al.*, 1998; Schmitz *et al.*, 2001; Mercer *et al.*, 2006; Chorev & Brecht 2012).

Models which account for SPW-Rs assuming axonal gap junctions were suggested in earlier works (Draguhn *et al.*, 1998; Traub *et al.*, 1999; Traub & Bibbig 2000; Traub *et al.*, 2012) and can account for spikelets, the fact that spikes during sharp wave are antidromic (i.e. arise in axons; Papatheodoropoulos 2008; Bähner *et al.*, 2011), the high temporal and spatial synchrony of PC spiking, and other *in vitro* data mentioned above. Other models, which explain SPW-Rs only by chemical synapses, address neither the *in vitro* nor *in vivo* data adequately (see Discussion). Confidence in the axonal origin of ripples is increased by two additional pieces of evidence, both related to the predicted high firing rates of axonal compartments (Traub *et al.*, 2012). First, there are high-frequency trains of sharp wave-associated synaptic currents, in CA1 PCs and CA1 oriens lacunosum-moleculare interneurons (INs) (which receive little synaptic excitation from CA3) (Maier *et al.*, 2011; Pangalos *et al.*, 2013). Second, in a related model of gamma oscillations, also dependent on axonal coupling (Traub *et al.*, 2000, 2003), the prediction of frequent axonal firing concurrent with less frequent somatic spikes has been directly verified with simultaneous axonal and somatic recording (Dugladze *et al.*, 2012).

Recent *in vivo* patch clamp recordings from behaving rats demonstrated that spikelets are common in PCs in CA1 during exploration and waking rest (Harvey *et al.*, 2009; Epsztein *et al.*, 2010) and under anesthesia (Chorev & Brecht 2012). Spikelet occurrence is highly correlated with the animal's position in the place field of the recorded cell (Epsztein *et al.*, 2010), during both exploration and immobility. This suggests that spikelet incidence is modulated by sensory (presumably synaptic) input to the PC during theta and SPW-R events. How can synaptic input in dendrites possibly modulate the incidence of spikelets, which seem to originate from the axon? To our knowledge, there are no biophysical models that can address this question.

Here, we propose a model of ripples, in which the incidence of ripples (and antidromic spikes) is modulated by synaptic input in the dendrites of PCs. Small changes in somatic potential gate spike propagation from an axonal collateral to the main axon, so that EPSPs can turn on, and inhibitory post-synaptic potentials can turn off ripple-associated somatic spikes. Using this mechanism, we demonstrate the ripple-associated replay of PCs, thus suggesting a new explanation for place cell reactivation. We also discuss possible application of the synaptic gating to the recent puzzling experiments (Lee *et al.*, 2012), where small somatic depolarizations turned a silent PC into a place cell.

Materials and methods

CA1 pyramidal cells

We used the model of a CA3 pyramidal neuron (Traub *et al.*, 1994) with the following ionic currents: fast sodium [Na(F)], potassium delayed-rectifier, potassium transient current, potassium after-hyperpolarization, Ca-dependent and voltage-dependent potassium current, and high-threshold Ca current. The high-threshold Ca conductance was reduced by twofold compared with the CA3 model, in order to avoid excessive bursting typical for CA3 pyramids and to make the firing pattern more similar to CA1. Somato-dendritic conductance densities were as described in Traub *et al.* (1994), except for lower somatic Na(F) (0.070 S/cm^2), to ensure that only few spikelets become somatic spikes (Epsztein *et al.*, 2010). The ionic conductance densities were uniform in all axonal compartments [axonal initial segment (AIS), main axon and collaterals]: Na(F), 0.3 S/cm^2 and potassium delayed-rectifier, 0.4 S/cm^2.

The dimensions of the axonal compartments were: AIS: length, 40 μm; diameter, 2 μm; main axon: length, 210 μm; diameter, 1 μm; collaterals: length, 200 μm; diameter, 0.5 μm. The two collaterals branched out of the main axon, at distances 50 μm (proximal) and 150 μ*m* (distal), respectively, from the soma (Fig. 1A). The geometrical ratio of collateral diameters to the main axon is defined by 3/2 power law (Rall 1959): $GR = (d_{main}^{3/2} + d_{main}^{3/2})/d_{collat}^{3/2} = 5.66$. This value, in our model, is greater than 1, which suggests a high failure probability of spike propagation from the mother branch to both daughter branches (for review see Debanne 2004). The mother branch in our case is the proximal collateral, whereas the daughter branches are the proximal and distal portions of the main axon.

The membrane capacitance was 0.75 μF/cm^2 for all compartments, membrane resistance (R_m) was 5×10^4 Ωcm^2 for soma-dendrites and 10^3 Ωcm^2 for axonal compartments. The cytoplasmic resistance (R_a) was 200 Ωcm for soma-dendrites and 100 Ωcm for axonal compartments. The reversal potentials were: leak current, −65 mV in all compartments; sodium reversal potential, 50 mV in all compartments; and potassium reversal potential, −80 mV in soma-dendrites compartments and −90 mV in axonal compartments (Traub *et al.*, 1994). The AMPA reversal potential was 0 mV. Somata were tonically hyperpolarized by −0.05 nA, and AIS by −0.1 nA, to prevent propagation of spikes from proximal collateral to the main axon, under resting conditions.

Electrotonic length constants

The passive cable electrotonic length constant $\lambda = \sqrt{aR_m/2R_a}$ was 2500 μm for the apical dendritic shaft, 1768 μm for proximal basal dendrites, 223 μm for the AIS, 158 μm for the main axonal trunk. The latter two values of axonal length constant are significantly smaller than the 700 μm estimated from experiments in mossy fibers (Alle & Geiger 2006). This suggests that the effect of dendritic EPSPs may reach more distally along the axon, and the affected axon-collateral branching point can be even further away from the soma than assumed in our simulations.

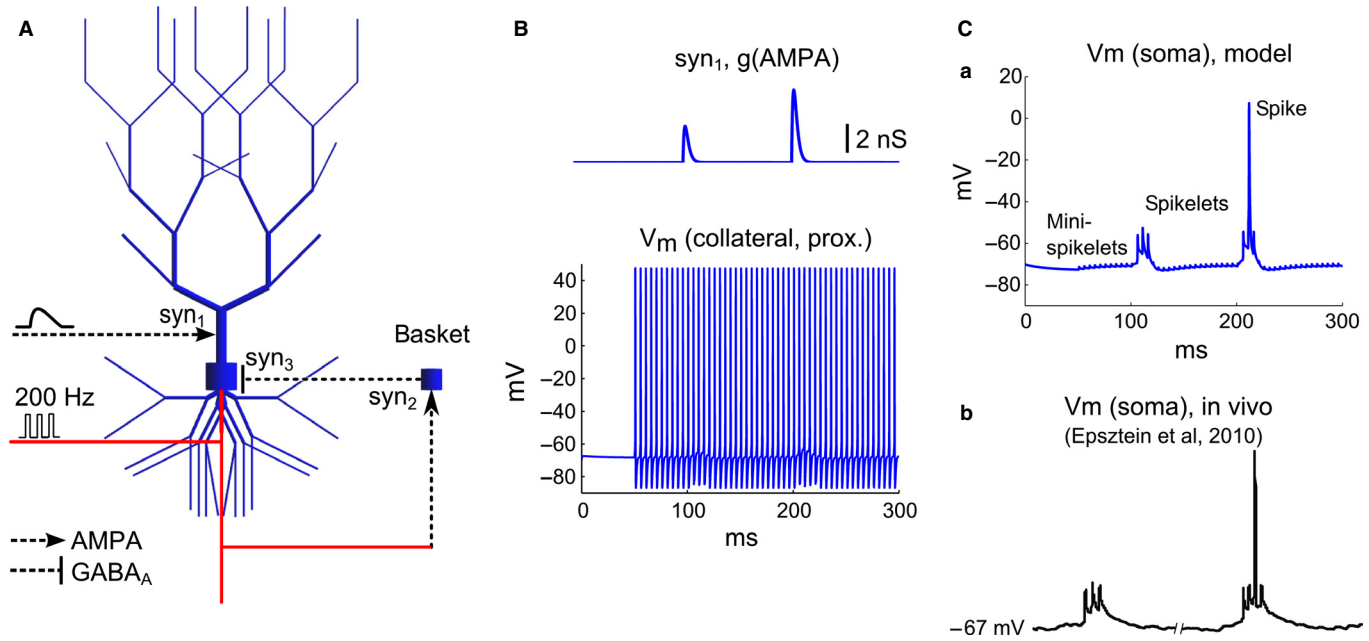

FIG. 1. Somatic spikelets gated by dendritic EPSPs. (A) The CA1 pyramidal neuron with inhibitory feedback from a basket cell (1 PC + 1 IN model). The axon is shown in red. The proximal axonal collateral of the pyramidal neuron receives current pulses at 200 Hz to imitate ongoing high-frequency activity in the axonal network interconnected by gap junctions. The apical dendrite receives external EPSPs at syn1 (AMPA). The distal axonal collateral projects to the IN via syn2 (AMPA), which in turn projects back to the soma of the pyramidal neuron via syn3 ($GABA_A$). (B) The PC receives two EPSPs (at 100 and 200 ms, respectively, time axis as in lower panel), whereas its proximal axonal collateral is tonically active with firing frequency of 200 Hz (starting at 50 ms). (C) (a) The axonal collateral activity remains hidden at the level of the soma (mini-spikelets), but the two EPSPs unmask this hidden activity and trigger bursts of somatic spikelets and occasional spikes. (b) For comparison, two parts of a single *in vivo* recording from a CA1 pyramidal neuron in a behaving rat [from Epsztein *et al.* (2010), reprinted with permission from AAAS]. Time and voltage scales are equal in (a) and (b).

Interneuron (fast-spiking)

This cell type was simulated as a one-compartment cell (Wang & Buzsáki 1996) with Na(F) (0.035 S/cm^2) and potassium delayed-rectifier (0.009 S/cm^2) conductances, R_m of 10^4 Ωcm^2, membrane capacitance of 1 μF/cm^2, dimensions of length, 20 μm and diameter, 20 μm. The reversal potentials were leak current, −65 mV; potassium reversal potential,−90 mV and sodium reversal potential, 55 mV.

Synaptic connections

The AMPA synaptic conductance time course was alpha-function $g = g_{max}(t/\tau)\exp(-(t-\tau)/\tau)$, which reaches maximum conductance g_{max} at time τ from the onset. The parameters were: pyramidal-to-pyramidal AMPA synapses: g_{max}, 5 nS; τ, 2 ms; pyramidal-to-basket synapses: g_{max}, 3.5 nS; τ, 0.8 ms; afferent 'cue' synapse to Pc: g_{max}, 2.5 or 5 nS (as indicated); τ, 2 ms; reversal potential E_{rev}, 0 mV for all. PCs projected to their post-synaptic targets via the distal axonal collateral.

The $GABA_A$ synapses from INs to PCs were simulated with double-exponential conductance time course $g_{max}(\tau_2/\tau_2-\tau_1)(-\exp(-t/\tau_1)+\exp(-t/\tau_2))$, which reaches g_{max} at time $\tau_1\tau_2 \log(\tau_1/\tau_2)/(\tau_1-\tau_2)$ after the onset. The parameters were τ_1, 2 ms; τ_2, 5 ms; E_{rev},-75 *mV*; and peak conductance g_{max}, 30, 40 or 50 nS (as indicated). The $GABA_A$ synapses were located at the center of the PC soma.

One pyramidal cell + one interneuron model

A PC received excitation from an afferent AMPA synapse (syn1) positioned on its apical shaft, 25 μm from the soma. This synapse performed gating of the antidromic APs arriving from the proximal axonal collateral. The PC projected to an IN via another AMPA synapse (syn2, g_{max} 3.5 nS). This AMPA synapse is strong enough to make the IN follow the pre-synaptic APs nearly 1 : 1. The IN projects back to the soma of the PC via a strong $GABA_A$ synapse (syn3, 50 nS), which represents combined feedback from many INs rather than a unitary inhibitory post-synaptic potential.

Sixteen pyramidal cell + one interneuron model

Pyramidal cell no. 0 received excitation from an afferent AMPA synapse ('cue' EPSP), which was equivalent to syn1 in the 1 PC+1 IN model. We assume that some AMPA synapses were formed (potentiated) between CA1 PCs during preceding theta oscillations via long-term potentiation, as suggested in Skaggs *et al.* (1996). A total of two AMPA synapses (5 nS each) were set between PCs, connecting cell nos. 0→1 and 1→2. These two AMPA synapses were positioned on basal dendrites of the PCs, 35 μm from somata (path distance), and performed gating of antidromic spikes in the corresponding PCs (nos. 1 and 2).

All PCs projected to a single IN via AMPA synapses (3.5 nS). The IN (effectively representing a number of INs lumped together) projected back to the soma of each PC via strong $GABA_A$ synapses (30 nS).

Forward replay network: eighty-one pyramidal cells + nine interneurons model (a network of nine clusters, each with nine pyramidal cells + one interneuron)

Pyramidal cell no. 0 received excitation from an afferent AMPA synapse ('cue' EPSP) as in the 1 PC+1 IN model. We assume that

some AMPA synapses were formed (potentiated) between the PCs, as in the 16 PC+1 IN model, with a total of four AMPA synapses (5 nS each), connecting cells that belong to different clusters: no. 0 → 3, 3 → 30, 30 → 33, and 33 → 60.

Each PC projected to the IN in its cluster via an AMPA synapse (3.5 nS). The IN projected back to the soma of each PC within its cluster via a strong $GABA_A$ synapse (50 nS). Inhibitory connections were local (within the cluster), whereas excitatory connections were across clusters.

Forward and reverse replay network: eighty-one pyramidal cells + nine interneurons model

This network was analogous to the Forward replay network, with the following modifications. Five new excitatory synapses were added, which connected the PCs in reverse order: 60 → 33, 33 → 30, 30 → 3, and 3 → 0. The new excitatory synapses were set identically to existing ones; the distal axonal collateral of the pre-synaptic PC projected to a basal dendrite of the post-synaptic PC. The peak conductance of excitatory synapses was the same (3.5 nS). The inhibitory $GABA_A$ synapses from INs were stronger (70 nS).

Gap junction connections and ripple generation

In the 1 PC+1 IN model, no actual gap junctions were present. The network-driven effect of gap junctions (i.e. ripples) was emulated by injecting pulses of current into the distal end of the proximal axonal collateral (0.05 nA, t_{on}, 1 ms; t_{off}, 4 ms; which gives 200 Hz). This pattern of stimulation corresponds, approximately, to what a randomly chosen PC axon would 'see' from population activity of its electrically coupled neighbors; random stimulation of individual axons produces emergent periodic oscillations of the network, if the network is sufficiently large (Traub *et al.*, 1999 2012).

We do not assume any specific synaptic targets for these proximal collaterals; they may project to different subtypes of INs, which then would experience ripple frequency excitatory synaptic drive during SPW-Rs (Pangalos *et al.*, 2013).

In the other network models (16 PC + 1 IN and 81 PC + 9 IN), each proximal axonal collateral had three gap junctions that were randomly positioned between 0.25 and 0.75 of its length. Gap junctions of different collaterals were interconnected in a random (regular) network, with the probability of connection independent of the distance between cells. No self-connections were allowed, but double connections between the collaterals of two different cells were possible. We chose a connectivity of three gap junctions per cell and regular network (constant number of connections per cell) to ensure that all cells are electrically coupled, and no cells are isolated. Synchronous activity in a network with more sparse connections is also possible, because as little as 1.5 gap junctions/cell in an Erdös-Rényi type of network ensures that most cells will be coupled into a giant component network (Traub *et al.*, 1999).

Gap junctions were non-rectifying and voltage-independent, with a conductance of 3 nS in all simulations shown, but other conductances (2–10 nS) can also be used. Conductances below 3 nS increase phase jitter between axonal (and somatic) spikes and make trans-junctional propagation prone to failures, which can lead to high-frequency re-entrant activity in large networks (Vladimirov *et al.*, 2012). Conductances higher than 3 nS increase the network firing frequency by sending reflected spikes from the soma back into the collaterals (Traub *et al.*, 1999).

Sixteen pyramidal cell + one interneuron model

The ripple-frequency network activity was elicited by semirandom stimulation (NEURON's NetStim.noise, 0.5) of the distal ends of the proximal axonal collaterals (0.05 nA, 1 ms, ∼100 Hz each). Once a collateral was stimulated, all other collaterals in the network fired an AP within a 0.5–1.0 ms interval; the activity of the collaterals' network was thus highly synchronous, with a mean frequency of ca. 250 Hz, in agreement with previous models (Traub *et al.*, 1999).

Eighty-one pyramidal cell + nine interneuron model

The gap junction connection method was the same as above, with connections allowed between axon branches of PCs lying in different clusters. Collaterals were stimulated randomly (0.05 nA; 1 ms; on average every 20 ms per collateral; Poisson time intervals, i.e. NetStim.noise, 1; ∼50 Hz on average).

Availability

The model is available at http://senselab.med.yale.edu/modeldb/ShowModel.asp?model=150446.

Results

Before proceeding to the simulation results, we highlight our model assumptions. We assume that certain collaterals of pyramidal axons are connected to each other via gap junctions; this assumption is motivated by the observations that sharp-wave-associated APs are antidromic (Papatheodoropoulos 2008; Bähner *et al.*, 2011), and that ripples can occur with chemical synapses blocked (Draguhn *et al.*, 1998). In contrast to earlier models, which assumed gap junctions on axonal trunks or distal branches (Traub *et al.*, 1999; Traub & Bibbig 2000; Traub *et al.*, 2012), we assume that gap junctions are present only between proximal collaterals, and those collaterals originate from the main axons not too far from the somata (∼ 50 μm). High-frequency oscillations (of order 200 Hz) can be generated in such an axonal plexus via random (and rare) ectopic spikes in participating axons, due to the propagation of synchronization waves though the network of axons (Traub *et al.*, 1999). In the oscillating plexus, axonal compartments near gap junction sites oscillate at, or near, the network frequency, i.e. ∼200 Hz (Traub *et al.*, 1999, 2012). Physically, then, one can imagine a randomly chosen neuron, in the system, as having its axon see a phasic input at ∼200 Hz, which results from the emergent network activity. We let this activity be present for long periods (hundreds of ms).

The main concept of our model is the following: due to tonic hyperpolarization of the AIS (Dugladze *et al.*, 2012), the spikes in the proximal collateral fail to propagate into the main axon, unless peri-somatic regions of the cell are synaptically depolarized. When, for example, an afferent EPSP arrives in a dendrite, the AIS becomes depolarized by a few mV. Such a depolarization of the AIS allows the main axon, near the proximal branching point, to reach threshold, and the collateral spikes start to propagate into the main axon. In this way, a chain of excitatory synaptic links can produce a replay sequence, even though somatic APs are antidromic.

Synaptic gating at axonal branch: one pyramidal cell + one basket cell

To illustrate the concept, we simulate a pyramidal neuron with an afferent AMPA synapse (syn1) and an axon with two branching

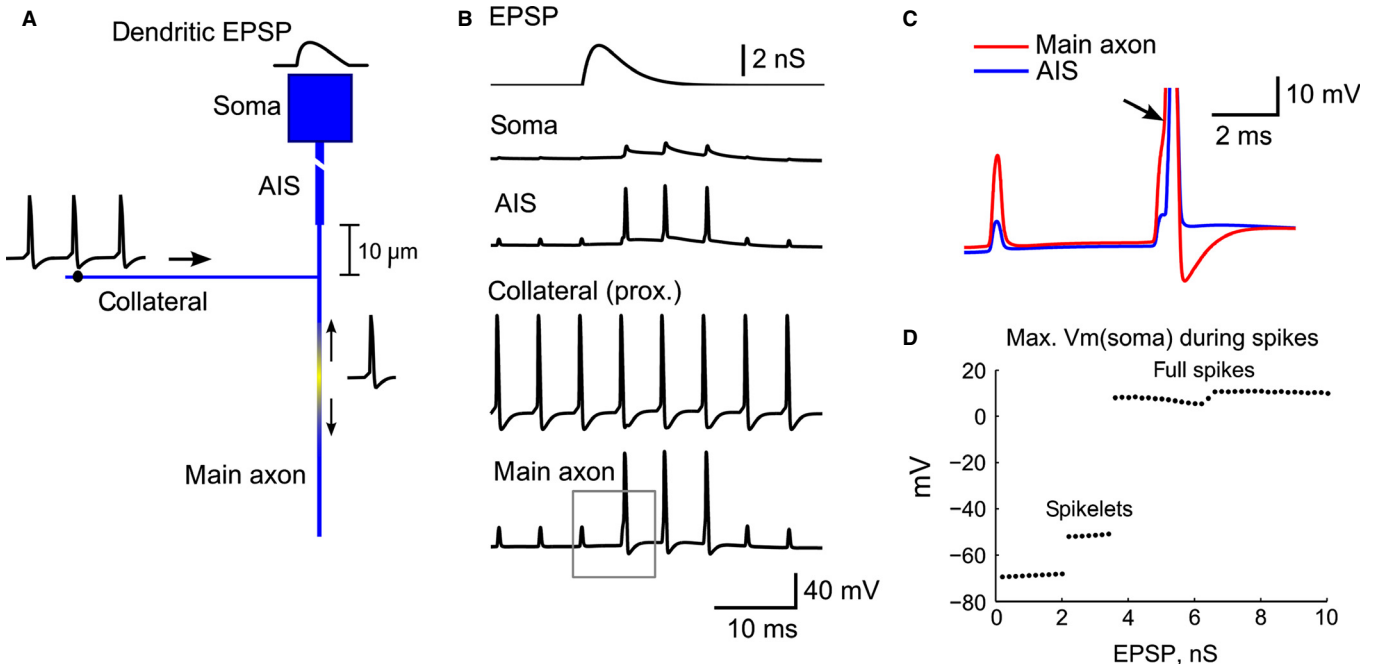

FIG. 2. Synaptic control of antidromic spike propagation into the main axon. (A) Close-up view of the spike initiation zone. After the dendritic EPSP onset, an AP from the proximal collateral invades the main axon and initiates an AP distally (initiation zone shown by yellow segment, ca. 20 μm distal to the branching point, shown at the time of spike maximum). Axonal Vm color coded: blue, −70 mV; yellow, +40 mV. The axonal AP propagates both antidromically (arrow up) and orthodromically (arrow down). The proximal collateral, AIS and main axon are truncated. (B) The course of EPSP conductance along with membrane potentials of the soma, AIS, proximal collateral, and main axon. All plots are temporally aligned. In each compartment, Vm was measured at its center, except the main axon (20 μm distal from the branch point). (C) The time interval of the first axonal spike in B (gray box) is shown in more detail. The moment when voltage in the main axon crosses the firing threshold is shown by the arrow, and it precedes the AP in the AIS by 0.2 ms. Spikes are truncated. (D) Peak voltage during spikes elicited by EPSPs of different amplitude (changed by increments of 0.2 nS), showing that spikelets are all-or-none phenomena.

points (Fig. 1A). The first axonal collateral (proximal to soma) receives brief current pulses at 200 Hz in its distal tip, to imitate the emergent activity in the axonal plexus. These high-frequency current injections will be replaced by a combination of gap junctions and random pulses with lower frequency in network models in subsequent sections. The second (distal) axonal collateral just projects to the basket cell via an AMPA synapse (syn2). Activity in the distal collateral follows activity in the main axon, so that, in this case, the distal collateral is not critical for ripple generation *per se*, although it is critical for producing recurrent inhibition.

External inputs to the pyramidal neuron are shown in Fig. 1B; they consist of two dendritic EPSPs and the ongoing 200 Hz activity in the proximal axonal collateral. As shown in Fig. 1C(a), spikes in the proximal collateral are barely visible in the soma as small high-frequency voltage deflections ('mini-spikelets', amplitude <1.5 mV), insufficient to elicit somatic spikes. When, however, the PC receives a dendritic EPSP (syn1, g_{max}, 2.5 nS; onset at 100 ms), the soma fires a burst of spikelets. When a stronger EPSP is applied (5 nS; onset at 200 ms), one somatic spikelet becomes a full spike along with several spikelets. The transition from mini-spikelets to full APs (spikelets or spikes) does not result from somatic depolarization *per se*, but from secondary depolarization of the axon (see below).

The full spikes have a shoulder on the rising phase, formed by a spikelet (Fig. S1). As shown in earlier models (Traub *et al.*, 1999) and in experiments (Hu *et al.*, 2009), somatic spikelets can occur as AIS APs that fail to propagate fully into soma.

The simulated somatic membrane potential is notably similar to patch-clamp recordings in behaving rats (Epsztein *et al.*, 2010) [reproduced in Fig. 1C(b)], both qualitatively and quantitatively. The spikelets start abruptly and are grouped in bursts on top of a slow depolarizing envelope. In our model, the spikelet amplitude was 10.98 ± 1.00 mV (mean ± SD, $n = 5$), in good agreement with the data of Epsztein *et al.* (2010) (amplitudes of 10–15 mV were reported, Fig. 1E in that article). In our simulations the spikelet 10–90% rise time (0.18 ± 0.01 ms, mean ± SD) was faster than the experimental value of Epsztein *et al.* (2010) (0.56 ± 0.08 ms, mean ± SEM), possibly because of the simplified model of the soma-AIS region, but it is within a range reported in Mercer *et al.* (2006) (0.10–0.80 ms).

Importantly, neither EPSPs nor high-frequency mini-spikelets alone are able to elicit APs in the soma. Indeed, axonal integration of peri-somatic EPSPs with subthreshold axon-collateral firing is key to the behavior of this model. In the absence of antidromic spikes, the simulated EPSPs depolarize the soma by 1.7 and 3.3 mV, respectively, far from firing threshold (∼18 mV above baseline, −73 mV, the cell being tonically hyperpolarized). The mini-spikelets are also small (<1.5 mV). Only when the EPSP is added onto the background of high-frequency mini-spikelets do they become somatic spikelets or spikes. The relevant site of integration, however, is not in the soma itself, but rather at the first axonal branch point. The location of the excitatory synapse can be anywhere on the dendritic tree, provided sufficient excitation at the proximal axonal branch point is produced; in this simulation the location was on the apical shaft.

The mechanism of the described somatic bursting is determined in the model by conduction failure/success at the first axonal branch point. The APs in the proximal collateral repeatedly fail to elicit APs in the main axon, but the axon remains close to the threshold. When peri-somatic regions of the cell are depolarized by an EPSP, the membrane near the first branching point of the axon also depolarizes (Fig. 2). Although the EPSP is small, it causes a

sufficiently strong depolarization in the main axon, due to the small diameter and high impedance, and brings the axon closer to threshold. Spikes from the collateral start to propagate into the main axon, and appear at the soma as spikelets and occasional full spikes. The APs repeatedly initiate in the main axon, not in the AIS, because the main axon is closer to firing threshold than is the AIS due to the collateral activity (Fig. 2C). With some delay (imposed by syn2 and syn3), the inhibitory IN quenches the axonal activity by peri-somatic inhibitory post-synaptic potentials, with an effect opposite to the EPSPs, blocking conduction at the branching point. An absence of inhibitory feedback sends the pyramidal neuron into continuous seizure-like firing. Stronger dendritic depolarization and weaker inhibitory feedback can increase the number of spikes and spikelets in the burst.

The onset time of an afferent EPSP does not have to be aligned with the timing of collateral spikes, because a typical EPSP has a time course (rise + decay) substantially longer than one ripple cycle (ca. 5 ms), so that there is at least one guaranteed collateral spike during an EPSP.

Ripples with forward replay: sixteen pyramidal cells + one interneuron network

The minimum circuit of one PC and one IN, described above, can be generalized to simulate a ripple with replay in a small, idealized network (Fig. 3).

We simulated a network of 16 PCs and one IN. The proximal collaterals of PCs are randomly coupled by gap junctions (three gap junctions/collateral), and the distal tips of the proximal collaterals are randomly stimulated by current injections, at about 100 Hz (see Materials and methods for justification of this protocol). All PCs project to a single IN, which projects back to the somata of all PCs. PC nos. 0, 1 and 2 are connected synaptically into a chain; the distal collateral of cell i projects onto a basal dendrite of cell i + 1 via an AMPA-receptor synapse. The distal collateral of a connected cell will only fire if a spike in the proximal collateral is able to invade the main axonal trunk. In this way, an EPSP on one cell in the chain can be permissive for the development of an EPSP in the next cell in the chain, the basis of replay.

Cell no. 0 receives an afferent ('cue') EPSP in its apical shaft (5 nS; onset at 20 ms) and fires a burst, providing EPSPs to cell no. 1. The latter starts bursting with some delay (peak to peak, 4.1 ms) on the next cycle of the ripple (Fig. 3B). Cell no. 2 fires only a burst of spikelets, without full spikes, due to high somatic hyperpolarization. All three PCs fire in phase with each other (phase jitter < 1.0 ms), driven by the shared quasi-periodic activity in the axonal plexus. The rest of the 13 PCs that are not synaptically connected to any pyramidal neighbors (but axonally connected via gap junctions) remain silent at their somata, and become progressively hyperpolarized during the SPW-R.

The two dendritic AMPA synapses (connecting cell nos. 0 → 1 and 1 → 2) start their conductances phase-locked to the common ripple-frequency rhythm of the axonal plexus, so the corresponding excitatory post-synaptic currents (EPSCs) in PCs during the SPW-R are phase-locked to the troughs of ripple local field potential (Fig. 3C). The somatic inhibitory post-synaptic currents triggered by the pre-synaptic basket cell are also phase-locked to ripples by the same mechanism, but delayed from pyramidal neuron firing (and local field potential troughs) by ca. 2 ms, due to the synaptic delays of syn2 and syn3. This is consistent with the experimental findings that both EPSCs and inhibitory post-synaptic currents in PCs are phase-locked to ripples, and EPSCs precede inhibitory post-synaptic currents (Maier *et al.*, 2011).

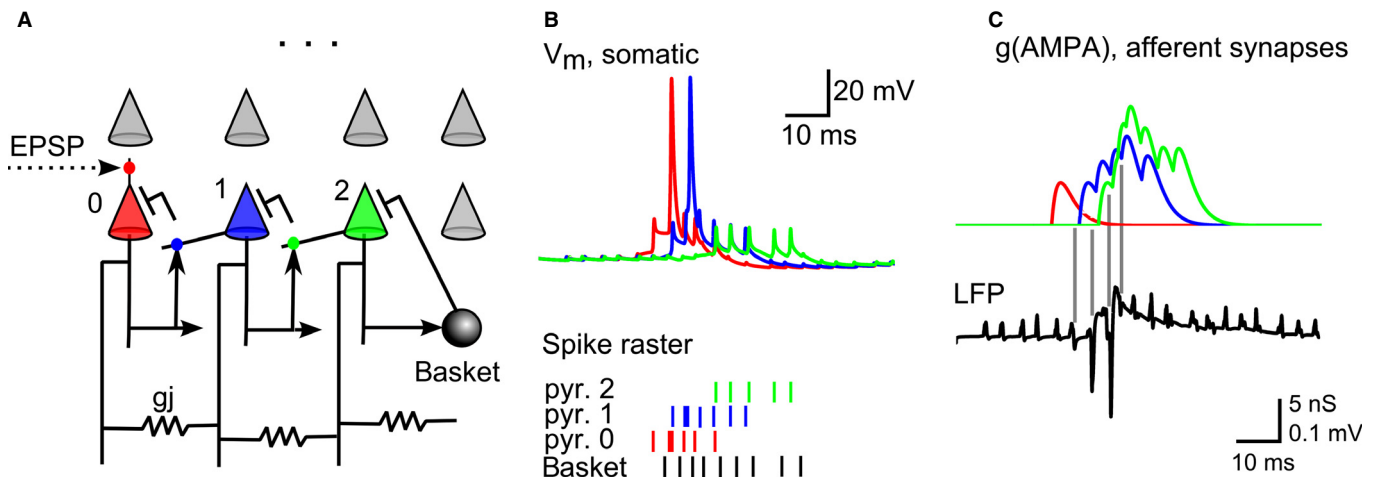

FIG. 3. Ripples with replay in a small network. (A) A network of 16 PCs (eight shown) and one IN (16 PC + 1 IN model). Proximal collaterals of pyramidal neurons were coupled in a random network by gap junctions (gj) and stimulated with random current pulses (Materials and methods). The distal collateral of cell i projects to a basal dendrite of cell i + 1 (i = 0, 1) via an AMPA synapse (arrows). Cell no. 0 receives the afferent ('cue') EPSP in its apical dendrite, and starts replay of the synaptically connected sequence (nos. 0, 1, 2). All PCs project to the basket cell (sphere) via AMPA synapses (arrows). The basket cell projects back to all PCs via peri-somatic inhibitory synapses (blunt arrows). The typical connectivity is shown on cell no. 2. (B) Somatic potentials of the cells participating in the replay. The onset of post-synaptic cell no. 1 firing occurs at the next ripple cycle from pre-synaptic cell no. 0 (firing starts from a spikelet). When cells fire concurrently, their spikes have high temporal coherence (< 1 ms jitter). Lower panel: raster plot of the three replayed cells along with the basket cell. Both spikelets and spikes are shown (bars for spikes are thicker). The basket cell is repeatedly delayed by ca. 2 ms due to synaptic delays of syn2 and syn3 [compare with (Ylinen *et al.*, 1995; Traub & Bibbig 2000)]. (C) Conductances of the two dendritic excitatory synapses are phase-locked to the trough of ripple local field potential (LFP) (blue for cell no. 1, green for cell no. 2 synapse, red for the 'cue' synapse in cell no. 0). Simulation is the same as in B. Phase-locking occurs due to the common pacemaker mechanism of spiking provided by the axonal plexus. The $GABA_A$ conductances are similarly phase-locked to the ripple. Phase-locking of synaptic conductances is in agreement with Fig. 6C in Maier *et al.* (2011). Gray lines show the time points of LFP troughs during the ripple.

Feedback inhibition to all pyramidal somata increases because the basket cell fires following somatic firing of any one PC. This, in turn, hyperpolarizes the somata of all PCs, both the participating (i.e. with somatic firing during the SPW-R) and non-participating ones, as seen in previous experiments (Maier *et al.*, 2003).

The time interval between the firing of the first synaptic pair (cells nos. 0 and 1) is relatively robust against parameter variation, and normally happens on consecutive ripple cycles. This is not the case for the second synaptic pair (cells nos. 1 and 2) because cell no. 2 starts late during the SPW-R and is inhibited more strongly. In most simulations, cell no. 2 missed one to three ripple cycles before the onset of a spikelet. Robust replay here could be simulated only for the first pair of PCs. How can longer sequences, of many cells, be replayed during an SPW-R? We address this question in the next simulation.

Forward replay in a large network (eighty-one pyramidal cells + nine interneurons)

We here assume that PCs are synaptically connected to a common IN in local clusters of the size of nine PCs per one IN (9 PC + 1 IN). Our global network consisted of nine such clusters, with the following assumptions: axons of PCs are connected globally (via gap junctions, as before); the distal tips of the proximal collaterals are randomly stimulated by current injections, at about 50 Hz; INs receive and project locally within a cluster; and PCs can be connected synaptically in sequences of any length, within or between clusters, but with no more than two PCs in series from the same cluster. This latter assumption prevents the development of excessive synaptic inhibition in participating cells and makes replay more precise in time.

As shown in Fig. 4, replay of a long sequence (five cells) can be reproduced in this network. As in the smaller network, the timing of PC somatic firing is temporally locked to the ripples, and each post-synaptic cell starts firing on the next ripple cycle from its pre-synaptic neighbor. The somatic APs (spikelets and spikes) of successive cells are temporally aligned and they occur synchronously, in consecutive cycles of the ripple rhythm.

Forward and reverse replay in a large network (eighty-one pyramidal cells + nine interneurons)

By adding five new excitatory synapses that coupled the PCs in reverse order, we were able to simulate both forward and reverse replays of the five-cell sequence (Fig. 5), accompanied by SPW-R-like events in the simulated extracellular field potential (similar to Fig. 4C). It is remarkable that recurrent excitatory connections between pre-synaptic and post-synaptic neurons do not prevent accurate replay in any one specified direction [the replay direction is determined by the cell that fires first, rather than by the unidirectionality of synapses (which are essentially symmetric here)]. The forward synaptic connections are active during reverse replay, but they activate later than reverse connections, so the spiking sequence is determined by those that activate first.

The total excitatory current received by each PC was higher than in the forward-only model, because of positive feedback loops between the neurons; firing of a post-synaptic neuron excited the pre-synaptic neuron. The uncontrolled bursting of cells was prevented by using stronger inhibitory feedback from the basket cells [g(GABA) = 70 nS instead of 50 nS].

Key model parameters

The SPW-R model that we propose depends, of course, on parameters. The model tolerates some changes in cellular geometry: length and diameter of axonal compartments, and position of the proximal branching point. The ion channel conductances and kinetics can also be varied across a reasonably wide range. The key parameters in our model are:

(i) proximity of the axonal branch to the soma/AIS, diameter of the proximal collateral, AIS hyperpolarization, and Na(F) (transient

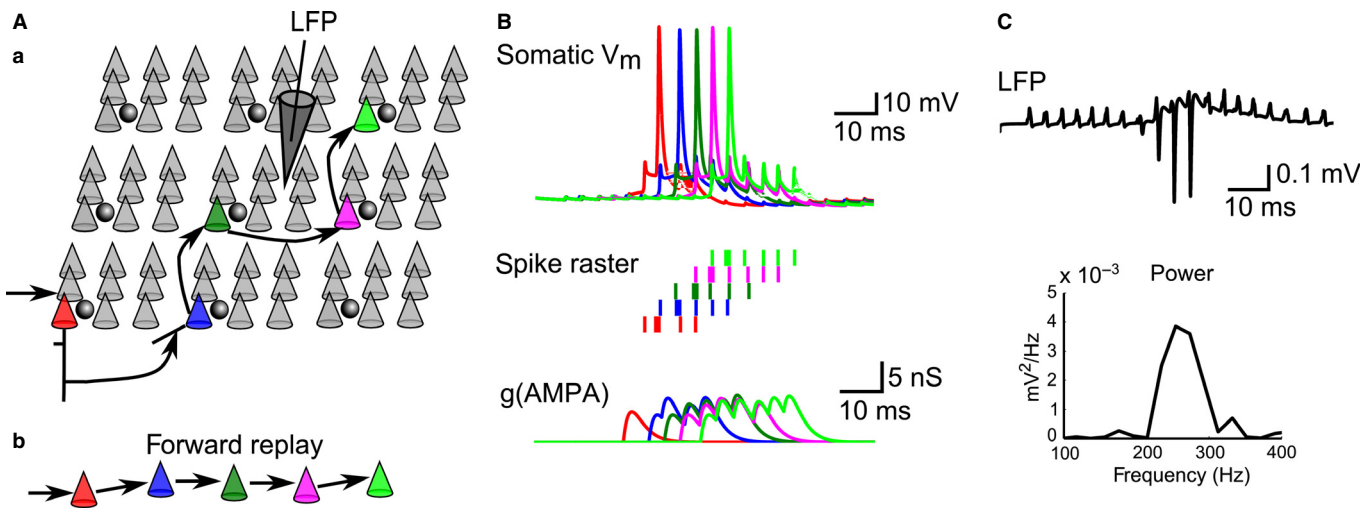

FIG. 4. SPW-R with cell replay in a larger network. (Aa) The network consists of nine clusters of nine PCs and one IN each (81 PC + 9 IN model). INs (basket cells) are shown as spheres. Proximal collaterals of PC axons are connected by gap junctions in a random network, and stimulated by current pulses randomly (see Materials and methods). Distal collaterals of four PCs (colored) each project to a basal dendrite of another PC, and form a synaptic chain (shown by arrows, b). (B) A 'cue' EPSP in the apical dendrite of the red cell triggers a replay of the five connected cells at ripple frequency. Cells belong to different clusters, but they are globally interconnected by axonal gap junctions, which ensures temporal coherence of spikes. Dendritic EPSCs are also temporally coherent (lower panel). (C) The extracellular field potential recorded near the center of the network ('electrode' position is shown in A). Small upward potentials reflect spikes in the axonal plexus. Deep negative potentials reflect somatic spikes of cells that are close to the 'electrode' (last three cells in the chain). Slow upward wave reflects peri-somatic inhibitory post-synaptic potentials. Lower panel: power spectrum of the local field potential (LFP) after high-pass filtering (cut-off 100 Hz). Compare B and C with Diba & Buzsáki (2007).

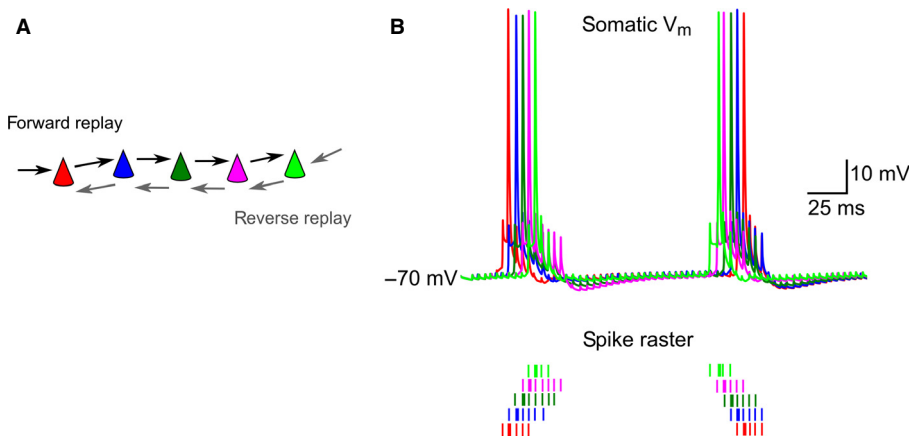

FIG. 5. SPW-R with forward and backward replay. The network is similar to the one shown in Fig. 4, but five new AMPA synapses are added (gray arrows in A), which allow reverse replay of the PC sequence. The somatic voltage of participating cells is shown in B. Initiation of forward replay is triggered by the afferent AMPA synapse to the red cell. Reverse replay is initiated after 130 ms by an afferent synaptic input to the green cell. Both events are driven, as before, by sub-threshold synchronous activity in the axonal network, which provides tight spiking synchrony of PCs (B, lower panel).

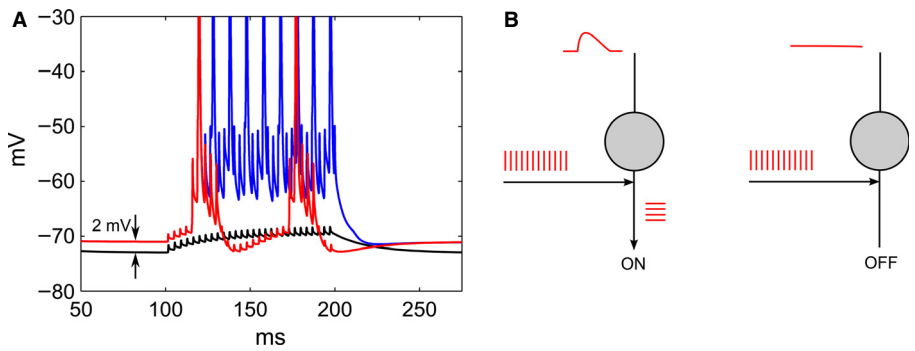

FIG. 6. Small somatic depolarizations can turn a PC on/off. (A) Depolarization of PC resting potential by 2 mV can turn a silent cell into a firing one. Depolarization of somatic resting potential by 2 mV (current injection, 0.04 nA, onset at 0 ms) changed the cell spiking mode from silent (black) to firing (red or blue, with the mode depending on the strength of inhibitory feedback, see the main text). Spikes are truncated. (B) The model of a PC has some analogy to a transistor, where somatic depolarization works as a gate voltage, the proximal collateral as a source, and the main axon as a drain of APs. When an EPSP is present, the axonal spikes are on, otherwise they are off. Note that the collaterals are electrically coupled to each other and provide a synchronous 'clock' at 200 Hz. See Materials and methods and Discussion.

Na^+) conductance at the branch area; all of these parameters contribute to spike failure/propagation from the proximal collateral into the main axon; and

(ii) somatic hyperpolarization, which determines the number of somatic spikes/spikelets in a burst of a PC.

We studied the phase space of the system 1 PC + 1 IN by varying selected pairs of the most important parameters (Fig. S3), and confirmed that the predicted phenomenon of dendritic EPSPs gating the antidromic APs is relatively robust against parameter variations.

Small somatic depolarizations can activate the cell

A direct consequence of our model is that a small depolarization of the PC resting potential can turn a silent cell into a firing cell, provided there is a hidden activity in its proximal axonal collateral. We simulated a model equivalent to that shown in Fig. 1, but spikes in the proximal axonal collateral were elicited by long step current injection (0.035 nA, onset at 100 ms, duration 100 ms) (instead of regular pulses, although either of the two protocols is valid). Depolarization of the somatic resting potential by 2 mV (current injection, 0.04 nA) changed the cell spiking mode from silent to firing (Fig. 6A). The silent cell (black line) demonstrates only mini-spikelets, which can be masked by noise in the real recordings. The firing mode can be tonic or bursting, depending on the strength of GABAergic feedback from the basket cell [g(GABA) = 20 nS for tonic firing (blue), and g(GABA) = 40 nS for bursting (red)]. Notice the slow depolarization 'hill' and presence of spikelets in both firing modes. This, in principle, suggests a putative mechanism for the enigmatic effect of a small somatic depolarization that is capable of turning a silent PC into a place cell (Lee *et al.*, 2012), although some unresolved questions remain (see Discussion).

Discussion

We suggest a model of SPW-Rs that: (i) allows synaptic modulation of SPW-R onset and duration; (ii) accounts for synchronous replay of PCs at ripple frequency in the CA1 region with its sparse excitatory recurrent synaptic connections; and (iii) accounts for the antidromic nature of PC action potentials, as required by *in vitro* and *in vivo* data (discussed below). The critical structural and dynamic basis of the model consists of two features: (i) the ripple-frequency firing of selected axonal compartments, consistent with experimental observations of ripple-frequency synaptic currents in CA1 pyramidal neurons and INs (Maier *et al.*, 2011; Pangalos *et al.*, 2013); and (ii)

the synaptic gating of spike invasion from an axon collateral into the main axon.

Our model suggests that the proximal axonal branching point in neurons can perform synaptic integration, if there is spontaneous activity in the collateral that otherwise fails to propagate into the main axon. Subthreshold dendritic EPSPs and the (by themselves) failing collateral spikes may together bring the branching point to threshold before the rest of the axon, whereas peri-somatic inhibitory post-synaptic potentials can reverse the effect. This allows the precise synaptic control of SPW-R onset and termination, as well as control of somatic firing times.

We extended the earlier models of SPW-Rs (Traub *et al.*, 1999; Traub & Bibbig 2000) to account for the following experimental data.

(i) PC somata fire bursts of spikes and spikelets of apparently antidromic shape, during active exploration and rest, as recorded by patch clamp in awake behaving rats (Epsztein *et al.*, 2010).
(ii) Despite their apparent antidromic origin, the incidence of those spikes and spikelets depends on sensory input within the place field (Epsztein *et al.*, 2010).
(iii) Place cell sequences are replayed during SPW-Rs at ripple frequency, and their somata prefer to fire phase-locked to the local field potential (Diba & Buzsáki 2007).
(iv) The replay sequence reflects recent experience (place fields visited by the animal), suggesting that plasticity in chemical synapses is crucial for SPW-R-associated replay (Wilson *et al.*, 1994; Skaggs *et al.*, 1996; Lee & Wilson 2002).
(v) In CA1, synaptic connectivity between PCs is sparse ($\sim$1%), and excitatory synapses are too weak to elicit APs in the post-synaptic PC by themselves (Deuchars & Thomson 1996). Nevertheless, SPW-Rs are recorded in isolated CA1 minislices (Maier *et al.*, 2003; Nimmrich *et al.*, 2005; Maier *et al.*, 2011), which prohibits input from other cortical regions.

Putative replay mechanism

The synaptic gating mechanism suggests a plausible model of forward replay of CA1 PCs during SPW-Rs *in vivo*. We hypothesize that during theta oscillations, some of the sparse excitatory synapses are formed or potentiated between place cells in CA1 (Skaggs *et al.*, 1996). During SPW-Rs, an afferent EPSP (a 'cue' stimulus) arrives at the first cell in the chain; the cell soma and axon then fire a burst of APs, which in turn then elicit EPSPs in its post-synaptic neighbor. These cells and their post-synaptic neighbors fire with precise timing due to ongoing, ripple-locked, synchronous activity ('clock') in the axonal plexus. That such a 'clock' can arise, emergently, in an electrically-coupled network of axons, has been shown in previous models (Traub *et al.*, 1999; Traub & Bibbig 2000).

Our model can in this way satisfactorily explain forward replay. Interestingly, the model can also explain reverse replay (Fig. 5), provided that synaptic 'chains' are allowed to run in opposite directions (i.e. a series of reciprocal excitatory synaptic links occurs), and that synaptic inhibition is sufficiently powerful during the SPW-R [as appears actually to be the case (Bähner *et al.*, 2011)].

Unexpectedly, our model also suggests a putative mechanism for the recent experiments of (Lee *et al.*, 2012), where the authors turned a silent PC into a place cell by a small depolarization of its somatic resting membrane potential (by 1–2 mV). In our simulation, depolarization of the somatic resting potential by 2 mV turned a silent cell into a firing cell (Fig. 6A), by unmasking the hidden activity in the axonal collateral. The model suggests a putative mechanism, but also poses new questions. In particular, the depolarization hill seen in the experiments is slow (seconds), and it emerges in all-or-none mode, even without somatic spikes (whereas the latter are required for the somatic depolarization hill in our model). The origin of the depolarization hill, dependent on the place field, remains unclear. Note, however, that the model presented here most specifically applies to SPW-Rs, rather than to the theta state, in which place cell recordings were made (Lee *et al.*, 2012).

Origin of antidromic activity

The origin of place field-specific spikelets seen in awake animals (Epsztein *et al.*, 2010) and simulated in our model via antidromic stimulation remains unknown. *In vitro*, distal axons can be excited by puffs of gamma-aminobutyric acid (GABA) (Bähner *et al.*, 2011), so that transient GABAergic tone can, in principle, initiate multiple antidromic spikes, and they may be global and synchronous due to the presence of axonal gap junctions. Although, in our model, such ectopic drive is global, only PCs that receive sufficient excitatory synaptic input participate in the SPW-Rs, due to the gating effects of EPSPs on axonal branch point conduction.

In the absence of sufficient synaptic excitation, the axon collateral activity in our model is seen as mini-spikelets in the soma (less than 1.5 mV in amplitude). This can make their detection difficult in actual *in vivo* recordings because of noise.

In Scheffer-Teixeira *et al.* (2012), high-frequency oscillations (140 Hz) were demonstrated during theta in CA1. The amplitude of these oscillations is low compared with SPW-Rs, but they are persistent during theta, and they reach maximal amplitude in the stratum oriens-alveus, where PC axons and basal dendrites both lie. These data are consistent with our model assumption about possible hidden activity in the proximal axons of PCs, but they need further experimental support (discussed below).

In our model of a PC, we adopt three novel assumptions: on axonal morphology, AIS hyperpolarization, and the location of gap junctions, which are discussed in the following three paragraphs.

Axonal morphology

Pyramidal cells in CA1 have an extensive axonal arbor with many collaterals (Scorcioni & Ascoli 2005). We assume that the axon bifurcates close to the distal end of the AIS (within 10 μm from the end of the AIS, whereas the AIS length itself may vary from 30 to 60 μm), and we assume that the collateral has a smaller diameter than the main axon. The axonal morphometry of CA1 PCs is still limited. Among three CA1 PCs with fully reconstructed axonal arbors (Scorcioni & Ascoli 2005) (NeuroMorpho.org; cell IDs: ca1a, ca1b and ca1c), one cell (ca1b) had a consistent distance (41 μm) from the start of its axon to its first branching point, whereas two other cells had much higher distances (139 and 125 μm). Cells from other reconstructions have very short axonal arbors and we are not sure that they adequately represent axonal branching as it would exist *in vivo*. Two of the three CA3 cells with fully reconstructed axonal arbors had their first branching point at 55 and 68 μm from the soma, respectively (cell IDs: ca3b-N2 and ca3pv-N4). These data indicate that axonal branching within the first 40–70 μm from the soma is not uncommon in both CA1 and CA3.

Axonal initial segment hyperpolarization

Pyramidal cells are hyperpolarized during SPW-Rs, at least *in vitro* (Bähner *et al.*, 2011). Peri-somatic hyperpolarization is likely because the somata of PCs receive mainly GABAergic synaptic

input from basket cells, which are highly active during SPW-Rs. Tonic AIS hyperpolarization (−0.1 nA in our model) is possible due to the presence of multiple GABAergic synapses on the AIS from axo-axonic cells (Buhl *et al.*, 1994), which have an inhibitory effect in CA3 and CA1 (Glickfeld *et al.*, 2008; Dugladze *et al.*, 2012), although they can be excitatory in the neocortex (Szabadics *et al.*, 2006; Woodruff *et al.*, 2009). Our assumption of a role for axo-axonic cells in regulating antidromic activity is consistent with the recent data of Dugladze *et al.* (2012). Hyperpolarization of the AIS in our model results in conduction failure from the proximal collateral into the main axon at the branch point. Propagation failures at axonal branching points are known in many species and neuron types (reviewed in Debanne 2004).

Plexus of proximal axonal collaterals

We assume in our model that some proximal collaterals can be coupled by gap junctions to form a network (axonal plexus), a network capable of fast synchronization and the generation of network oscillations at ripple frequency (Traub *et al.*, 1999). The assumption of an axonal plexus is supported by several lines of evidence. High-frequency field oscillations in the CA1 stratum oriens were demonstrated when it was physically isolated from PC bodies (Traub *et al.*, 2003). Ripple-frequency EPSCs in CA1 PCs and oriens lacunosum-moleculare INs were demonstrated during *in vitro* SPW-Rs (Maier *et al.*, 2011; Pangalos *et al.*, 2013). These EPSCs are likely to derive from the ripple-frequency firing of PC axons.

In our model, due to conduction failures at the axonal branching points, the plexus of axonal collaterals may sustain activity at near ripple frequency for long periods (seconds), without significant effects on somatic and extracellular voltages. A biological precedent exists in the hippocampus for the dissociation between axonal and somatic PC firings, with the axons firing significantly more than somata; during persistent gamma oscillations (Dugladze *et al.*, 2012).

Our model suggests that small somatic depolarizations can control the propagation of spikes from the plexus into the main axon of a cell. This mechanism is different from the one proposed in Munro & Kopell (2012), where somatic potential regulates the conduction of a spike across a gap junction. Here, gap junction conductance is presumed secure, and what is regulated is the branch point propagation.

Ambiguity of the term 'pyramidal cell spiking'

In the light of our model and *in vivo* recordings (Epsztein *et al.*, 2010), the definition of spiking of PCs becomes somewhat ambiguous. *In vivo*, there are somatic spikes and spikelets, both appearing to result from full APs in the axon. Additionally, in our model, an AP in the main axon is different from an AP in the collateral. Therefore, throughout this article, we distinguish five types of spikes: somatic mini-spikelet, spikelet, spike [Fig. 1C(a)], axonal spike, and collateral spike. We believe that some extracellular recordings (Buzsáki *et al.*, 1992) may not capture somatic spikelets generated in PC somata because of their low amplitude, and because the thresholds for spike detection are somewhat arbitrary. Therefore, several spikes recorded extracellularly during SPW-Rs may actually correspond to both spikelets and somatic spikes (Chorev & Brecht 2012).

Interneuron spiking

Interneurons fire multiple APs throughout SPW-Rs, at ripple frequency, as shown *in vivo* by intracellular and extracellular recordings (Buzsáki *et al.*, 1992; Ylinen *et al.*, 1995; Klausberger *et al.*, 2003), as well as intracellular recordings *in vitro* (Bähner *et al.*, 2011). Our model reproduces the frequent spiking of INs during the SPW-R, and the phase delay of INs by 2–3 ms relative to the pyramidal somatic spikes/spikelet (and corresponding local field potential troughs), due to the synaptic delay from PCs to INs (Traub & Bibbig 2000). INs provide essential negative feedback; without it, a single EPSP in our model triggers a cascade of epileptiform bursting in PCs, as observed *in vitro* after pharmacological $GABA_A$ receptor blockade (Maier *et al.*, 2003).

Axonal myelination

In our model, we simulated the unmyelinated axons of PCs. The axons of PCs in CA1 alveus are most likely myelinated by oligodendrocytes (Yamazaki *et al.*, 2007). However, it is unclear how distally myelination starts, and its extent may be age-dependent (Arnold & Trojanowski 1998). We therefore simulated cells with myelinated axons, where myelination starts 10 μm distally from the end of the AIS (and the branching point of the proximal axonal collateral). We found that our main result, synaptic gating, also holds for this case (Supporting Information, Fig. S3). The PCs with myelinated axons require smaller somatic and AIS hyperpolarization (−0.05 and −0.02 nA, respectively), but stronger dendritic EPSPs (at least 5 nS) to reproduce the effect of synaptic gating.

Memory encoding

The model suggests that memories can be stored in CA1 as chains of place cells unidirectionally connected by excitatory synapses. The EPSPs generated in such chains are, by themselves, subthreshold for eliciting APs, but store temporal relations between place cells. The memory sequence can then be retrieved by synaptic ('cue') stimulation of the first cell in the chain, which triggers the cell replay at ripple frequency, driven by antidromic axonal activity. Cells that do not belong to the stimulated chain(s) remain silent during the SPW-R event, so that the total somatic network activity remains low. Our model suggests that spatio-temporal information between place cells can be stored and retrieved in very sparse synaptic networks. With approximately 320 000 PCs in rat CA1 (Boss *et al.*, 1987) and synaptic connectivity of 1%, the total number of recurrent synapses within CA1 can be still extremely large ($320\,000 \times 3200 \sim 10^9$). The memory capacity of such a network is beyond the scope of the present article, but it is an interesting question for further work.

Analogy with a transistor

The proposed mechanism of synaptic gating, if valid, suggests that a PC can, under certain conditions, act like a transistor (Fig. 6B). Synaptic depolarization at the soma can act as a gate voltage, which controls the propagation of spikes from the proximal axonal collateral (source) to the main axon (drain). After passing the axonal branching point, the spikes propagate to downstream targets of the axon. Small changes in the somatic potential turn the trains of axonal spikes on/off, controlling the spike timing and their number in the main axon. Note that the collaterals ('sources') are electrically coupled to each other and thus provide a synchronous 'clock' of the network at ripple frequency. Connecting such cells into chains and trees can provide a substrate for cell replay. In the case of a tree-like structure, the activation of one cell can trigger the activation of two or more alternative replay sequences. The inhibition of alternative sequences by INs may control which branch is replayed.

Possible experiments for model validation

The most precise experiment would involve the recording/stimulation of proximal collaterals and concurrent stimulation of synapses on a proximal dendrite of a PC to detect if synaptic gating of an axonal branch indeed takes place. However, this experiment may be too difficult technically. A readily testable experimental prediction would be the following: although the blockade of glutamate receptors may not suppress rippling (Nimmrich *et al.*, 2005) (which is assumed to be generated by the axonal plexus), the blockade should strongly influence which somata fire *in vivo*, as our model proposes that somatic firing is modulated by fast EPSPs. Thus, adding an AMPA/kainate receptor blocker may, *in vivo*, turn cells participating in ripples (Bähner *et al.*, 2011) into non-participating ones. Conversely, drugs that can enhance or prolong AMPA receptor-mediated currents, such as cyclothiazide, should cause increased somatic firing [as in Fig. 1C(a)].

We can make two further predictions: (i) severing proximal collaterals can make the cell silent during SPW-Rs; and (ii) somatic APs should be more common in those CA1 PCs in which the axon projects out from a basilar dendrite, rather than the soma. EPSPs on the basilar dendrite, from which the axon projects, will more readily allow antidromic spikes to invade the soma. The labeling of patched cells (e.g. with biocytin) *in vivo* and accurate reconstruction of their proximal axonal morphology can possibly link the presence of spikelets with the axonal structure.

In a broader perspective, there is a crucial need for the experimental determination of: (i) which connexin or connexins are expressed in axons; and (ii) where on axons putative gap junctions are actually to be found. Gap junction blockers with high specificity are necessary for conclusive experiments.

Other models

Models of sharp-wave ripples based on chemical synapses

To the best of our knowledge, all alternative models of SPW-Rs with replay are based on recurrent networks with strong synaptic connectivity (Molter *et al.*, 2007; Koene & Hasselmo 2008). These models describe how encoding can be achieved via Spike-timing-dependent plasticity during theta oscillations with phase precession, and the stored sequences later replayed in SPW-Rs in either forward or reverse order using the strong recurrent synaptic connections.

In our present work, we adopt the first part of the above-mentioned models, which assumes theta-mediated encoding of place cell sequences, but suggest a different mechanism for SPW-R-associated forward replay. Models solely based on excitatory recurrent synaptic connections miss the temporally coherent ripple-frequency field oscillations because of variability in the firing latencies, due to the random number of afferent synapses per neuron in a random network (Traub & Wong 1982).

The model in Memmesheimer (2010) suggested that transient ripples can occur in a network of cells connected by supra-linear excitatory synapses. This mechanism is plausible in highly recurrent CA3, but not CA1, and does not address why ripples persist after the pharmacological blockade of excitatory synapses (Draguhn *et al.*, 1998).

A new type of SPW-R model was suggested in Taxidis *et al.* (2012), in which ripple-frequency oscillations in CA1 are generated by (fast) $GABA_A$ synaptic connections between INs alone. Although the model accounted for many experimental data, it remains unclear how this mechanism can generate ripples in the presence of the $GABA_A$ blocker bicuculline and in low-Ca medium, which does not permit synaptic transmission (Draguhn *et al.*, 1998); nor does it explain the antidromic nature of SPW-R-associated somatic APs.

Altogether, models that depend only on chemical synapses do not address the accumulated experimental data, i.e. sparse recurrent connections in CA1, persistence of ripples in non-synaptic conditions, antidromic shape of APs, and sensitivity to various gap junction blockers.

Models of sharp-wave ripples based on gap junctions

The model of SPW-Rs proposed in Traub & Bibbig (2000) used gap junctions between the main axonal trunks (263 μm from the soma) of PCs. The axons were stimulated by random ectopic spikes in their tips (by small current pulses) at low frequency, which resulted in high-frequency (140 Hz) oscillations of the axonal plexus. Sharp waves were produced by long (150 ms) excitatory synaptic conductances (afferent input) to PCs and INs, whereas concurrent ripples were generated by the axonal plexus. The model reproduced multiple experimental facts about SPW-Rs (Ylinen *et al.*, 1995): rare firing of PCs and frequent firing of INs; firing of different cell types, as well as synaptic currents phase-locked to ripples; PC somatic spikes having an antidromic shape, ripples being abolished when gap junctions were blocked, and other data.

The more recent model (Bähner *et al.*, 2011; Traub *et al.*, 2012) reproduced SPW-Rs driven by the axonal plexus, where gap junctions were positioned on distal axonal branches (180 μm from soma). This model reproduced rare antidromic spikes that arise from somatic hyperpolarization in participating neurons, and, importantly, nearly invisible spikelets as seen *in vitro* (but not *in vivo*). The model suggests that the distribution of the potassium transient current conductance in the proximal branching point of the axon can account for the observations *in vitro*. Models for *in vitro* and *in vivo* SPW-Rs can be different as the actual phenomena are, and in this work we specifically addressed *in vivo* SPW-Rs, which require spikelets but do not require somatic hyperpolarization before the neurons fire antidromic spikes.

All of the above-mentioned models (Traub & Bibbig 2000; Bähner *et al.*, 2011; Traub *et al.*, 2012) require specific modulation of either the spontaneous firing rate of axons in the plexus (Traub & Bibbig 2000) or the opening and closing of gap junctions in order to turn ripples on and off, which implies some as yet unknown step in plexus activity modulation. One possible mechanism was suggested in Munro & Kopell (2012); the somatic voltage can control spike propagation through gap junctions, if gap junctions are placed at the AIS or proximal main axon, but this mechanism appears not to work when gap junctions are located at collaterals. None of these models reproduced the replay of cells during SPW-Rs.

Our present model is different from the models summarized above in one key point. It allows the synaptic modulation of ripple onset and termination, via the EPSP-mediated control that is performed at the branching point of the collateral and the main axon. The synaptic gating mechanism on top of the axonal plexus 'clock' activity suggests a plausible model for the synchronous replay of place cells.

This article suggests a possible conceptual bridge between two currently opposing models of SPW-Rs, i.e. based on chemical synapses and based on gap junctions. We suggest that both mechanisms may act to amplify each other, and such a model can account for much of the available experimental data.

Supporting Information

Additional supporting information can be found in the online version of this article:

Fig. S1. Phase plots of the pyramidal cell spikes.

Fig. S2. Phase space of the model of synaptic gating.

Fig. S3. Model of pyramidal cell with myelinated axon.

Acknowledgements

We thank Jérôme Epsztein, Michael Brecht, and Edith Chorev for sharing their data and discussing the manuscript. We are grateful to Nikolaus Maier and Nelson Spruston for their suggestions on the manuscript. We also thank Albert Lee, Doyun Lee, Andreas Draguhn, Dietmar Schmitz, Tengis Gloveli and Tamar Dugladze for helpful discussions, and Ted Carnevale for his advice on NEURON programming. The work was supported by the following grants: NIH/NINDS (http://nih.gov) R01NS062955 (to N.V. and R.D.T.), R01NS44133 (to R.D.T.) and R01GM081747 (to Y.T.), and Alexander von Humboldt Stiftung (http://www.humboldtfoundation.de) and Einstein Stiftung Berlin (to R.D.T.).

Abbreviations

AIS, axonal initial segment; AMPA, alpha-amino-3-hydroxy-5-methyl-4-isoxazolepropionic acid; AP, action potential; EPSC, excitatory post-synaptic current; EPSP, excitatory post-synaptic potential; GABA, gamma-aminobutyric acid; $GABA_A$, gamma-aminobutyric acid type A; IN, interneuron; Na(F), fast sodium; PC, pyramidal cell; R_a, cytoplasmic resistance; R_m, membrane resistance; SPW-R, sharp-wave ripple.

References

Alle, H. & Geiger, J. (2006) Combined analog and action potential coding in hippocampal mossy fibers. *Science*, **311**, 1290–1293.

Arnold, S. & Trojanowski, J. (1998) Human fetal hippocampal development: I. Cytoarchitecture, myeloarchitecture, and neuronal morphologic features. *J. Comp. Neurol.*, **367**, 274–292.

Bähner, F., Weiss, E., Birke, G., Maier, N., Schmitz, D., Rudolph, U., Frotscher, M., Traub, R., Both, M. & Draguhn, A. (2011) Cellular correlate of assembly formation in oscillating hippocampal networks in vitro. *Proc. Natl. Acad. Sci. USA*, **108**, E607–E616.

Bendor, D. & Wilson, M. (2012) Biasing the content of hippocampal replay during sleep. *Nat. Neurosci.*, **15**, 1439–1444.

Boss, B., Turlejski, K., Stanfield, B. & Cowan, W. (1987) On the numbers of neurons on fields CA1 and CA3 of the hippocampus of Sprague-Dawley and Wistar rats. *Brain Res.*, **406**, 280–287.

Buhl, E., Han, Z., Lorinczi, Z., Stezhka, V., Karnup, S. & Somogyi, P. (1994) Physiological properties of anatomically identified axo-axonic cells in the rat hippocampus. *J. Neurophysiol.*, **71**, 1289–1307.

Buzsáki, G. (1986) Hippocampal sharp waves: Their origin and significance. *Brain Res.*, **398**, 242–252.

Buzsáki, G., Horvath, Z., Urioste, R., Hetke, J. & Wise, K. (1992) High-frequency network oscillation in the hippocampus. *Science*, **256**, 1025.

Chorev, E. & Brecht, M. (2012) In vivo dual intra and extracellular recordings suggest bi-directional coupling between CA1 pyramidal neurons. *J. Neurophysiol.*, **108**, 1584–1593.

Chrobak, J. & Buzsáki, G. (1996) High-frequency oscillations in the output networks of the hippocampal-entorhinal axis of the freely behaving rat. *J. Neurosci.*, **16**, 3056–3066.

Church, J. & Baimbridge, K. (1991) Exposure to high-pH medium increases the incidence and extent of dye coupling between rat hippocampal CA1 pyramidal neurons in vitro. *J. Neurosci.*, **11**, 3289–3295.

Csicsvari, J., O'Neill, J., Allen, K. & Senior, T. (2007) Place-selective firing contributes to the reverse-order reactivation of CA1 pyramidal cells during sharp waves in open-field exploration. *Eur. J. Neurosci.*, **26**, 704–716.

Davidson, T. J., Kloosterman, F. & Wilson, M.A. (2009) Hippocampal replay of extended experience. *Neuron*, **63**, 497–507.

Debanne, D. (2004) Information processing in the axon. *Nat. Rev. Neurosci.*, **5**, 304–316.

Deuchars, J. & Thomson, A. (1996) CA1 pyramid-pyramid connections in rat hippocampus in vitro: Dual intracellular recordings with biocytin filling. *Neuroscience*, **74**, 1009–1018.

Diba, K. & Buzsáki, G. (2007) Forward and reverse hippocampal place-cell sequences during ripples. *Nat. Neurosci.*, **10**, 1241–1242.

Draguhn, A., Traub, R., Schmitz, D. & Jefferys, J. (1998) Electrical coupling underlies high-frequency oscillations in the hippocampus in vitro. *Nature*, **394**, 189–192.

Dugladze, T., Schmitz, D., Whittington, M., Vida, I. & Gloveli, T. (2012) Segregation of axonal and somatic activity during fast network oscillations. *Science*, **336**, 1458–1461.

Ego-Stengel, V. & Wilson, M. (2010) Disruption of ripple-associated hippocampal activity during rest impairs spatial learning in the rat. *Hippocampus*, **20**, 1–10.

Epsztein, J., Lee, A., Chorev, E. & Brecht, M. (2010) Impact of spikelets on hippocampal CA1 pyramidal cell activity during spatial exploration. *Science*, **327**, 474–477.

Foster, D. & Wilson, M. (2006) Reverse replay of behavioural sequences in hippocampal place cells during the awake state. *Nature*, **440**, 680–683.

Girardeau, G., Benchenane, K., Wiener, S., Buzsáki, G. & Zugaro, M. (2009) Selective suppression of hippocampal ripples impairs spatial memory. *Nat. Neurosci.*, **12**, 1222–1223.

Glickfeld, L., Roberts, J., Somogyi, P. & Scanziani, M. (2008) Interneurons hyperpolarize pyramidal cells along their entire somatodendritic axis. *Nat. Neurosci.*, **12**, 21–23.

Hamzei-Sichani, F., Kamasawa, N., Janssen, W.G., Yasumura, T., Davidson, K.G., Hof, P.R., Wearne, S.L., Stewart, M.G., Young, S.R., Whittington, M.A., Rash, J.E. & Traub, R.D. (2007) Gap junctions on hippocampal mossy fiber axons demonstrated by thin-section electron microscopy and freeze–fracture replica immunogold labeling. *Proc. Natl. Acad. Sci. USA*, **104**, 12548.

Harvey, C.D., Collman, F., Dombeck, D.A. & Tank, D.W. (2009) Intracellular dynamics of hippocampal place cells during virtual navigation. *Nature*, **461**, 941–946.

Hu, W., Tian, C., Li, T., Yang, M., Hou, H. & Shu, Y. (2009) Distinct contributions of nav1. 6 and nav1. 2 in action potential initiation and backpropagation. *Nat. Neurosci.*, **12**, 996–1002.

Jadhav, S., Kemere, C., German, P. & Frank, L. (2012) Awake hippocampal sharp-wave ripples support spatial memory. *Science*, **336**, 1454–1458.

Klausberger, T., Magill, P.J., Márton, L.F., Roberts, J.D., Cobden, P.M., Buzsáki, G. & Somogyi, P. (2003) Brain-state-and cell-type-specific firing of hippocampal interneurons in vivo. *Nature*, **421**, 844–848.

Koene, R. & Hasselmo, M. (2008) Reversed and forward buffering of behavioral spike sequences enables retrospective and prospective retrieval in hippocampal regions CA3 and CA1. *Neural Netw.*, **21**, 276–288.

Kudrimoti, H., Barnes, C. & McNaughton, B. (1999) Reactivation of hippocampal cell assemblies: effects of behavioral state, experience, and EEG dynamics. *J. Neurosci.*, **19**, 4090–4101.

Lee, A. & Wilson, M. (2002) Memory of sequential experience in the hippocampus during slow wave sleep. *Neuron*, **36**, 1183–1194.

Lee, D., Lin, B.-J. & Lee, A.K. (2012) Hippocampal place fields emerge upon single-cell manipulation of excitability during behavior. *Science*, **337**, 849–853.

Maier, N., Nimmrich, V. & Draguhn, A. (2003) Cellular and network mechanisms underlying spontaneous sharp wave-ripple complexes in mouse hippocampal slices. *J. Physiol.*, **550**, 873–887.

Maier, N., Tejero-Cantero, Á., Dorrn, A., Winterer, J., Beed, P., Morris, G., Kempter, R., Poulet, J., Leibold, C. & Schmitz, D. (2011) Coherent phasic excitation during hippocampal ripples. *Neuron*, **72**, 137–152.

Memmesheimer, R. (2010) Quantitative prediction of intermittent high-frequency oscillations in neural networks with supralinear dendritic interactions. *Proc. Natl. Acad. Sci. USA*, **107**, 11092.

Mercer, A., Bannister, A.P. & Thomson, A.M. (2006) Electrical coupling between pyramidal cells in adult cortical regions. *Brain Cell Biol.*, **35**, 13–27.

Molter, C., Sato, N. & Yamaguchi, Y. (2007) Reactivation of behavioral activity during sharp waves: a computational model for two stage hippocampal dynamics. *Hippocampus*, **17**, 201–209.

Munro, E. & Kopell, N. (2012) Subthreshold somatic voltage in neocortical pyramidal cells can control whether spikes propagate from the axonal plexus to axon terminals: a model study. *J. Neurophysiol.*, **107**, 2833–2852.

Nádasdy, Z., Hirase, H., Czurkó, A., Csicsvari, J. & Buzsáki, G. (1999) Replay and time compression of recurring spike sequences in the hippocampus. *J. Neurosci.*, **19**, 9497–9507.

Nimmrich, V., Maier, N., Schmitz, D. & Draguhn, A. (2005) Induced sharp wave-ripple complexes in the absence of synaptic inhibition in mouse hippocampal slices. *J. Physiol.*, **563**, 663–670.

O'Keefe, J. & Nadel, L. (1978) *The Hippocampus as a Cognitive Map*. Oxford University Press, Oxford.
O'Neill, J., Senior, T. & Csicsvari, J. (2006) Place-selective firing of CA1 pyramidal cells during sharp wave/ripple network patterns in exploratory behavior. *Neuron*, **49**, 143–155.
Pangalos, M., Donoso, J.R., Winterer, J., Zivkovic, A.R., Kempter, R., Maier, N. & Schmitz, D. (2013) Recruitment of oriens-lacunosum-moleculare interneurons during hippocampal ripples. *Proc. Natl. Acad. Sci. USA*, **10**, 4398–4403.
Papatheodoropoulos, C. (2008) A possible role of ectopic action potentials in the in vitro hippocampal sharp wave-ripple complexes. *Neuroscience*, **157**, 495–501.
Rall, W. (1959) Branching dendritic trees and motoneuron membrane resistivity. *Exp. Neurol.*, **1**, 491–527.
Scheffer-Teixeira, R., Belchior, H., Caixeta, F., Souza, B., Ribeiro, S. & Tort, A. (2012) Theta phase modulates multiple layer-specific oscillations in the ca1 region. *Cereb. Cortex*, **22**, 2404–2414.
Schmitz, D., Schuchmann, S., Fisahn, A., Draguhn, A., Buhl, E., Petrasch-Parwez, E., Dermietzel, R., Heinemann, U. & Traub, R. (2001) Axo-axonal coupling: a novel mechanism for ultrafast neuronal communication. *Neuron*, **31**, 831–840.
Scorcioni, R. & Ascoli, G. (2005) Algorithmic reconstruction of complete axonal arborizations in rat hippocampal neurons. *Neurocomputing*, **65**, 15–22.
Skaggs, W.E., McNaughton, B.L., Wilson, M.A. & Barnes, C.A. (1996) Theta phase precession in hippocampal neuronal populations and the compression of temporal sequences. *Hippocampus*, **6**, 149–172.
Szabadics, J., Varga, C., Molnár, G., Oláh, S., Barzó, P. & Tamas, G. (2006) Excitatory effect of gabaergic axo-axonic cells in cortical microcircuits. *Science*, **311**, 233.
Taxidis, J., Coombes, S., Mason, R. & Owen, M. (2012) Modeling sharp wave-ripple complexes through a CA3-CA1 network model with chemical synapses. *Hippocampus*, **5**, 995–1017.
Traub, R. & Bibbig, A. (2000) A model of high-frequency ripples in the hippocampus based on synaptic coupling plus axon-axon gap junctions between pyramidal neurons. *J. Neurosci.*, **20**, 2086.
Traub, R. & Wong, R. (1982) Cellular mechanism of neuronal synchronization in epilepsy. *Science*, **216**, 745–747.
Traub, R., Bibbig, A., Fisahn, A., LeBeau, F., Whittington, M. & Buhl, E. (2000) A model of gamma-frequency network oscillations induced in the rat CA3 region by carbachol in vitro. *Eur. J. Neurosci.*, **12**, 4093–4106.
Traub, R., Schmitz, D., Maier, N., Whittington, M. & Draguhn, A. (2012) Axonal properties determine somatic firing in a model of in vitro ca1 hippocampal sharp wave/ripples and persistent gamma oscillations. *Eur. J. Neurosci.*, **36**, 2650–2660.
Traub, R.D., Jefferys, J.G., Miles, R., Whittington, M.A. & Tóth, K. (1994) A branching dendritic model of a rodent CA3 pyramidal neurone. *J. Physiol.*, **481**(Pt 1), 79–95.
Traub, R.D., Schmitz, D., Jefferys, J.G.R. & Draguhn, A. (1999) High-frequency population oscillations are predicted to occur in hippocampal pyramidal neuronal networks interconnected by axoaxonal gap junctions. *Neuroscience*, **92**, 407–426.
Traub, R.D., Cunningham, M.O., Gloveli, T., LeBeau, F.E.N., Bibbig, A., Buhl, E.H. & Whittington, M.A. (2003) GABA-enhanced collective behavior in neuronal axons underlies persistent gamma-frequency oscillations. *Proc. Natl. Acad. Sci. USA*, **100**, 11047–11052.
Vladimirov, N., Tu, Y. & Traub, R. (2012) Shortest loops are pacemakers in random networks of electrically coupled axons. *Front. Comput. Neurosci.*, **6**, 17.
Wang, X. & Buzsáki, G. (1996) Gamma oscillation by synaptic inhibition in a hippocampal interneuronal network model. *J. Neurosci.*, **16**, 6402–6413.
Wang, Y., Barakat, A. & Zhou, H. (2010) Electrotonic coupling between pyramidal neurons in the neocortex. *PLoS One*, **5**, e10253.
Wilson, M.A. & McNaughton, B.L. (1994) Reactivation of hippocampal ensemble memories during sleep. *Science*, **265**, 676–679.
Woodruff, A., Xu, Q., Anderson, S. & Yuste, R. (2009) Depolarizing effect of neocortical chandelier neurons. *Front. Neural Circuits*, **3**, 15.
Yamazaki, Y., Hozumi, Y., Kaneko, K., Sugihara, T., Fujii, S., Goto, K. & Kato, H. (2007) Modulatory effects of oligodendrocytes on the conduction velocity of action potentials along axons in the alveus of the rat hippocampal ca1 region. *Neuron Glia Biol.*, **3**, 325–334.
Ylinen, A., Bragin, A., Nádasdy, Z., Jandó, G., Szabo, I., Sik, A. & Buzsáki, G. (1995) Sharp wave-associated high-frequency oscillation (200 Hz) in the intact hippocampus: network and intracellular mechanisms. *J. Neurosci.*, **15**, 30–46.